MANSOURA JOURNAL OF Geology
Official Journal of Faculty of Science, Mansoura University, Egypt
E-mail: scimag@mans.edu.eg ISSN: 2974-4962

Assessment of geologic structures using integration of gravity measurements and digital elevation model, Ras Sudr area, Sinai, Egypt

Mona Metawee[1], Sultan A. S. Araffa[2], Amal Othman[1], Mohamed El Alfy[1]

1 Geology Department, Faculty of Science, Mansoura University, Mansoura 35516, Egypt.

2 National Research Institute of Astronomy and Geophysics (NRIAG), Helwan, Cairo 11421, Egypt.

Correspondence to: *mona.metawee95@gmail.com, +201009453053*

Received:20/2/2024
Accepted: 13/3/2024

Abstract: The current study was carried out in Ras Sudr area in the western part of Sinai which has attracted considerable attention due to several projects focusing on its growth and advancement. The initial purpose of this research involves utilizing DEM dataset and gravity data to evaluate and extract the surface streams and faults in addition to defining lineaments and assessing the uplifts and basins of the subsurface layers. By analyzing the Bouguer anomaly map, the gravity data's first horizontal and vertical derivatives using the Oasis Montaj program, the lineaments of the subsurface were successfully mapped. To differentiate between the deep and shallow sources from each other, an upward continuation technique was employed. The deep sources get smoother at 7 km below the surface. The determination of the causative body depth was identified by applying the downward continuation technique. Downward continuation maps change slightly from the original gravity data at 1000 and 1500 m, while the distortion of the map starts at 2000 m to 2500 m. DEM (Digital Elevation Model) data was downloaded from SRTM satellite images with 30-m resolution and analyzed in ArcGIS, mapping the stream segments over the area, and delineating the linear features from the hillshade map. There is a strong correlation found between the delineated lineaments from surface data and subsurface gravity data and this affects the configuration and movement of groundwater aquifers along the area. The rose diagrams for these lineaments were concluded and reflect the major trends that were distributed in the study area. NW-SE of the Gulf of Suez, N-S of Nile Valley, NE-SW of the Gulf of Aqaba, E-W of the Mediterranean Sea, and NEE-SWW of Syrian Arc System trends have affected the region. 2D and 3D gravity modeling were implemented through seven selected profiles indicating that the representative depth to the surface of the basement ranges from 2001 to 6069 m.

keywords: Gravity, Ras Sudr, Sinai, Structures, Modelling

1.Introduction

Ras Sudr is situated in the Gulf of Suez's eastern region and the southwestern part of Sinai, Egypt. It exhibits a significant capacity for the presence of hydrocarbon reserves and flashfloods which need to be highlighted to harness the area resources for use. The area of interest spans over about 4700 km^2 and is positioned between latitudes 29° 22´N and 29° 54´N as well as longitudes 32° 38´ E and 33° 39´E (Fig.1). This study objected to examine the characteristics and properties of the lineaments from the surface and the subsurface which can configure the underlying aquifers across the area. An integration between gravity data and SRTM data was carried out. The first objective of gravity surveying is to distinguish different kinds of rocks by detecting density irregularities from measurements of the attraction of gravity ([1]). Gravity data was utilized to define the subsurface lineaments and gravity inversion to indicate the basement's depth and the sedimentary units. Furthermore, the digital elevation model data was processed using spatial analysis tools and employed for flow direction, accumulation, and extracting the stream network within the area and mapping

the lineaments from the hillshade which was found to be the optimal map for extracting the geological linear features from the surface [2]. Several studies have been conducted in Sinai concerned with the geology, the hydrogeology, the geomorphology, and the hydrochemistry of this area ([3,4,5,6,7] However, in our present study, we will focus on extracting and defining the structural properties and trends that dissect the area from the surface and subsurface.

2. Geology

The region was geologically described from the geology map [8] which has a scale of 1:500,000 and the map was digitized and traced on ArcGIS software reflecting the different rocks which characterize Ras Sudr area (Fig. 2a). The area is bounded from the east by Egma, Al-Tih plateau and Sudr formation to the deposits of Quaternary and Miocene along the shoreline in west[9]. Quaternary sediments involve wadi deposits, sand dunes, fanglomerates, and alluvial hamadah deposits in the west and the upper northeast zones. Tertiary deposits were distributed over the area and mainly in the center, west zones, and Egma Formation in the east. These deposits from the upper Miocene to Paleocene include different formations such as Hamam Faraunal, Ayon Mosa, Kariem, and Belayem formations with evaporitic, limestone, and clastic deposits, while Rudays and Nukhul consist of conglomerates and sandstones. Eocene limestone deposits consist of Khaboba and Mokattam formations from the middle Eocene, Darat, and Minia formations with greyish white limestone from the lower-middle Eocene, and Thebes, Wasiyet, and Egma chalky limestone formations characterize lower Eocene deposits. Paleocene in the eastern section is represented by Greenish marly shale from Esna formation. Cretaceous sediments mainly occupy the eastern section and involve sediments from Maastrichtian which are remarked by Sudr chalk Formation with a higher distribution percentage of 20.1% over the area. Duwi and Matullah formations consist of classtics, carbonates, and limestone whereas Wata Formation from Turonian is represented by yellowish brown limestone intercalated with sandstone and shale in the middle. Finally, Malha Formation of kaolinized sandstone intercalated with conglomerate from Aptian-Albian. The stratigraphy corresponding the area is described as shown in the stratigraphic column (Fig. 2b). The tectonic events led to the presence of wadies, hills, and fault systems with different directions in the area[10].

3. Materials and methods

In this study the gravity measurements and DEM data refer to the digital elevation model data were implemented to identify the subsurface and surface structures features which distinguish the area. Gravity measurements were obtained over 174 observation stations using the Scintrex CG-3 Auto-grav (Automated Gravity Meter) by the Egyptian Geological Survey and Mining Authority (EGSMA). The gravity data were analyzed using [11] and subjected to upward and downward continuation filtering techniques, gravity derivatives in horizontal and vertical directions, and gravity modeling to highlight the subsurface anomalies and structure in addition to estimate the depth of sediment and to the basement rocks. While DEM data were collected from SRTM with 30-meter resolution through USGS. The analyses of the surface trends of the stream segments and hillshade map hold a significant importance in this study. These analyses were applied to the DEM data (Fig.3) and allow for a comparison between the subsurface tectonics and the surface topographical features, shedding light on the impact of subsurface fault structures on the surface stream segments that follow various paths within the study area in addition to delineating the linear features from the hillshade map using Image Analyst in (ArcGIS 10.8) and Line Module in (PCI Geomatica, 2016). DEM data was processed using Arc-Hydro tools and then utilized to define the stream network/drainage system of study area [12]. The map of the drainage system (Fig. 11) illustrates the stream segments of various paths that have been delineated within the study area. The delineated streams drain towards the Gulf of Suez except for a few streams in the northeastern zone flow towards the north. Moreover, the map illustrates that the drainage system over the area exhibits directions of NE-SW, NEE-SWW, and E-W.

4. Results and Discussion

4.1 Bouguer Gravity Anomaly Map

Different corrections were applied to the gravity data such as drift, tide, latitude, and elevation correction. Using this corrected gravity data the Bouguer Gravity Anomaly map has been constructed and it involves both regional and residual anomalies of deep and shallow sources, respectively. In (Fig. 4) the Bouguer anomaly map of the study area reveals that the gravitational field changes in the study area ranging from -52 to 5.6 mGal. The maximum values were distributed in southeastern, central, and northern zones while lower values were distributed in the western zones of the area.

4.2 Gravity Filtering Techniques

The upward continuation filtering technique is crucial for maximizing the gravitational effects of deeper gravity sources at the expense of anomalies caused by shallow sources[13]. Using the Oasis Montaj program, an upward continuation filtering approach that continued at 7000 m above the measuring level was applied to the gravity data. The gravity upward continued map at level 7000 m shows more smoothing features than others as shown in (Fig.5) has a maximum gravity value of -6.6 mGal at the southeastern, eastern, and northeastern parts of the study area and a minimum value of -44.7 mGal that decreases towards the southwest and west of the study area. Downward continuation is applied to improve the deep sources response by appropriately getting the plane of measurement closer to the source, (improving short-wave responses, this filter is referred to as a sharpening filter) [(14)]. Downward continuation maps were extracted at different depths of 1000, 1500, 2000, and 2500 m as shown (Fig. 6) and the complete distortion of the structure happens while increasing the depth gradually up to 2500 m. The downward continuation map of 2500 m showed that gravity field values range between 272.9 mGal to -300.4 mGal.

4.3 Gravity Derivatives

Gravity derivatives typically accentuate shallow sources and emphasize the edges and boundaries of gravity anomalies. Numerous methodologies are dedicated to identifying the edges and boundaries of gravity anomalies, specifically those generated by geological formations[15]. Currently, edge detectors are a crucial stage in interpreting gravity data[16]. In the current study, the first and second derivatives in the X, Y, and Z directions of the gravity anomaly map were delineated. The 1st dx showed that gravity values range between 1.54 mGal as a maximum value in NE, SW, south, and central part of the study area to -1.55 mGal minimum values in NW, SE, and northern zone of the study area. 1st dy reveals that the maximum value of gravity field was 0.0023 mGal distributed in the north, south, spot in the east and central parts of the study area while minimum values were -0.0027 mGal in the center, southeast, and spot in the southwest. 1st dz showed that the gravity values range between 0.0082 mGal as a maximum value to -0.0050 mGal as a minimum value, the high positive anomalies were found in the northwest, central parts, southeast, and northeast of the study area while lower values located in the west, east, spot in south and spot in the north. Also, second derivatives were delineated as shown in (Fig.7). The first horizontal derivative (FHD) and first vertical derivative (FVD) methods are widely employed to demarcate the boundaries of density variations from gravity values in order to identify the edges resulting from fault components or boundaries of rocks[17]. The maximum value of FHD serves as an indicator for delineating the structural elements while in FVD, the zero-contour line reflects the faults in the northwest and in the center of the area[18]. By analyzing the FHD map in X and Y directions, and the FVD map it showed that the faults/ lineaments in the study area exhibit NE-SW, E-W, NW-SE trends (Fig.10).

4.4 Gravity Modeling

Quantitative analysis of the potential gravity data was conducted from gravity modeling using GM-SYS (Oasis Montaj software, 2015). It was applied to identify the subsurface elements, the density characteristics and to calculate the basement surface depth over the region. Two-dimensional and three-dimensional gravity models were carried out at seven selected profiles (Fig.8). These selected profiles involve six horizontals toward the west-east direction with 73 km length and one vertical taking the south-north direction with 62

km length. Average gravity densities of 2.30 and 2.67 g/cm3 were applied to sedimentary and basement rocks; respectively[19]. The final deliverables from the 2D model were employed to create a 3D model and then the depth to the basement was calculated between 2.1 to 6.07 kilometers which coincides with the average depth from 2D (Fig.9).

4.5 Surface Analyses

Stream segments mapped in (Fig.11-C) exhibit various directions and locations. These segments can be classified into two major categories. The first one comprises stream segments that are influenced by subsurface faults and lineaments, indicating structural control in the area. The second category, which was naturally or physically controlled streams, consists of stream segments that are shaped by natural factors and conditions, such as erosion and weathering. The main trends of these streams are the Gulf of Suez, the Gulf of Aqaba, and the Syrian arc system. The rose diagram was created to illustrate the distribution of stream segments within the study area showing that the trend of NEE-SWW is the most predominant and has a stronger magnitude than other trends. Additionally, E-W and NE-SW trends have a higher magnitude than other trends. On the other hand, faults and lineament characteristics were extracted and mapped from hillshade layer, and the rose diagram of this layer reflects that the N-S, NE-SW, and NW-SE trends have a stronger magnitude than other trends (Fig.11-B).

5. Discussion

This current study was carried out in the Ras Sudr area in the western part of South Sinai and aims to enhance the comprehension of the structural conditions within the investigation area by examining both surface features and structure characteristics of the subsurface and their respective depths. Gravity measurements were employed for better representation of the subsurface and different techniques were used. The subsurface lineaments were extracted using the Bouguer anomaly map, the first horizontal derivatives maps in X and Y directions, and from the first vertical derivative map (Fig.10). After the statistical analyses for these maps, it has been concluded that the major trends within the area were NW-SE, N-S, NE-SW, E-W, and NEE-SWW. Gravity modeling was applied using seven profiles covering the area helping to calculate the depth of the basement rocks and sedimentary thickness revealing that the depth ranges from 2 km for the uplifts to 6.1 km for the basins. DEM data was analyzed effectively within the GIS environment to identify the structures from surface geology such as faults, and lineaments, as well as their impact on the stream network in the area. A significant number of the delineated streams over the area were influenced by the structural control category. These stream segments and lineaments were subjected to statistical analysis to define the major trends in this area. The rose diagram of stream segments reflects NEE-SWW, E-W, and NE-SW while the rose diagram of hill-shade map reflects N-S, NE-SW, and NW-SE trends. Therefore, there is a strong correlation between the extracted faults and lineaments from the surface and subsurface, indicating the extent of the faults from the subsurface to the surface. Moreover, these faults have a strong effect on the distribution of the surface water and groundwater aquifers and their configurations across the area of interest.

6. Conclusion

Both of surface and Subsurface analyses were applied over the study area to delineate the structure characteristics and lineaments that prevail in the area and affect the presence of hydrocarbons and groundwater resources. Potential gravity data and Digital elevation model data were analyzed to achieve the objective of this study. Different techniques were carried out to determine the dissecting trends of faults along the area using Bouguer anomalies, FHD, and FVD maps in addition to stream segments and hillshade maps. The trends that characterize the area are NW-SE of the Gulf of Suez, N-S of Nile Valley, NE-SW of the Gulf of Aqaba, E-W of the Mediterranean Sea, and NEE-SWW of Syrian Arc System trends. The upward continuation filtering technique was carried out at different distances of 3000, 4000, 6000, and 7000 m over the study area and reflects that the map become smoother at a depth of 7000 m. On the other hand, the downward continuation technique was applied at depths of 1000, 1500, 2000, and

2500 m and revealed that the full distortion happens at a depth of 2500 m. The gravity modeling reflects that the basement rocks exhibit a depth variation from 2 to 6.1 km where the eastern and south-eastern zones show the uplifts but western and north-western showing the basins of the area.

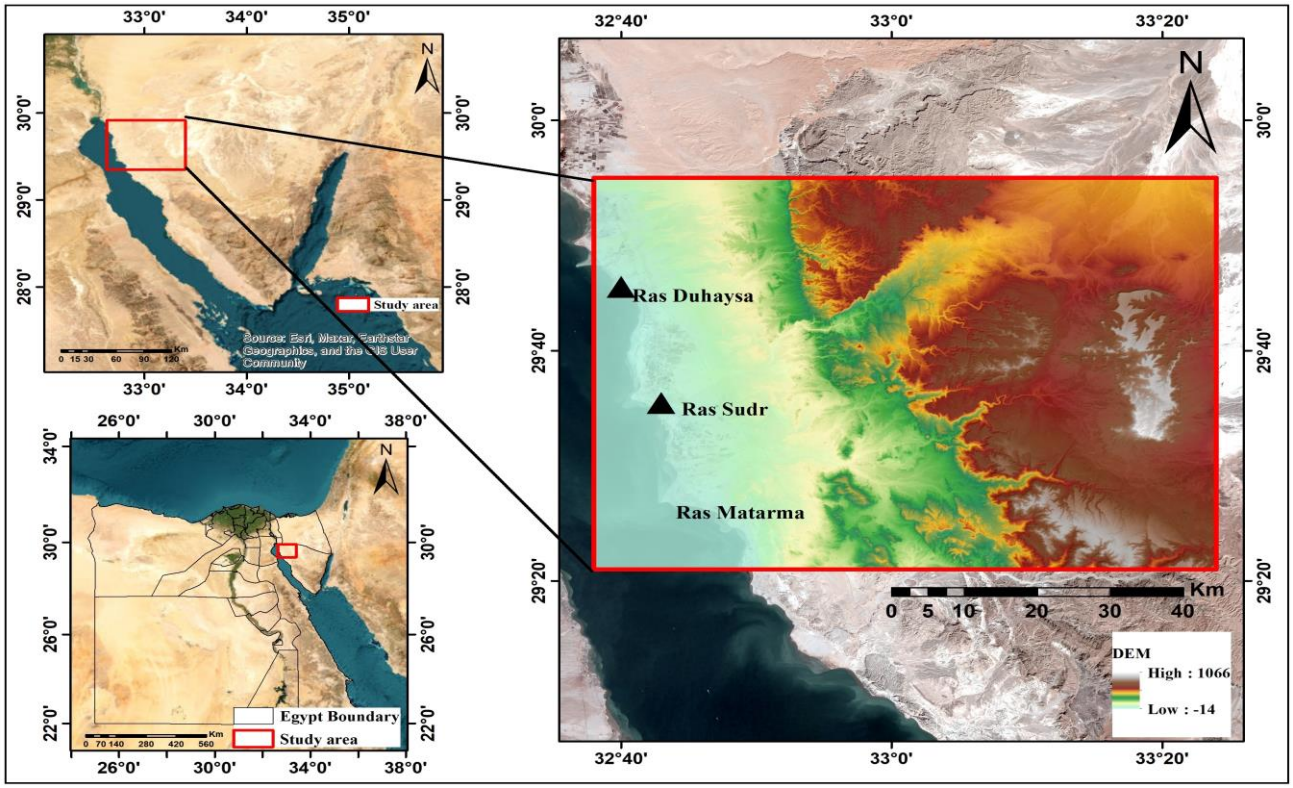

Fig.1: Location Map of the study area.

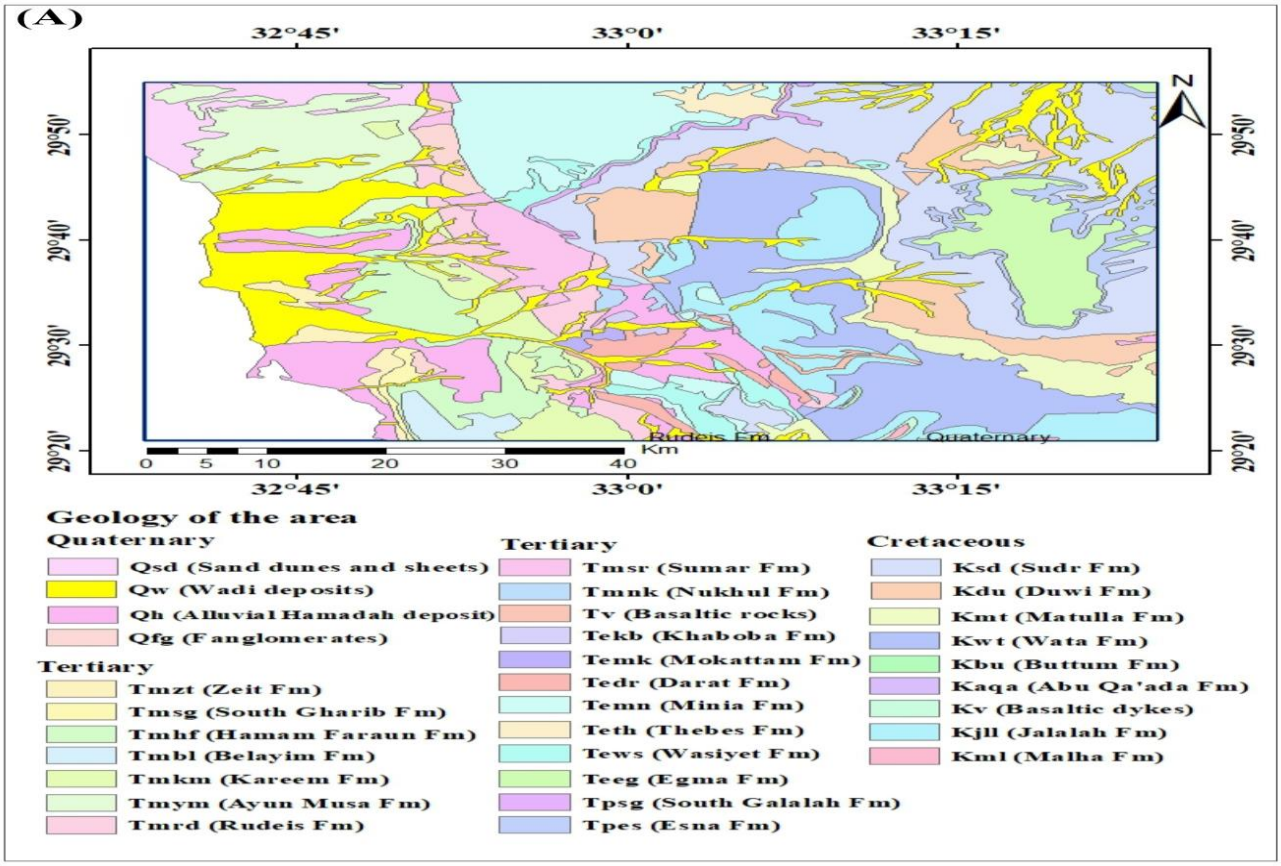

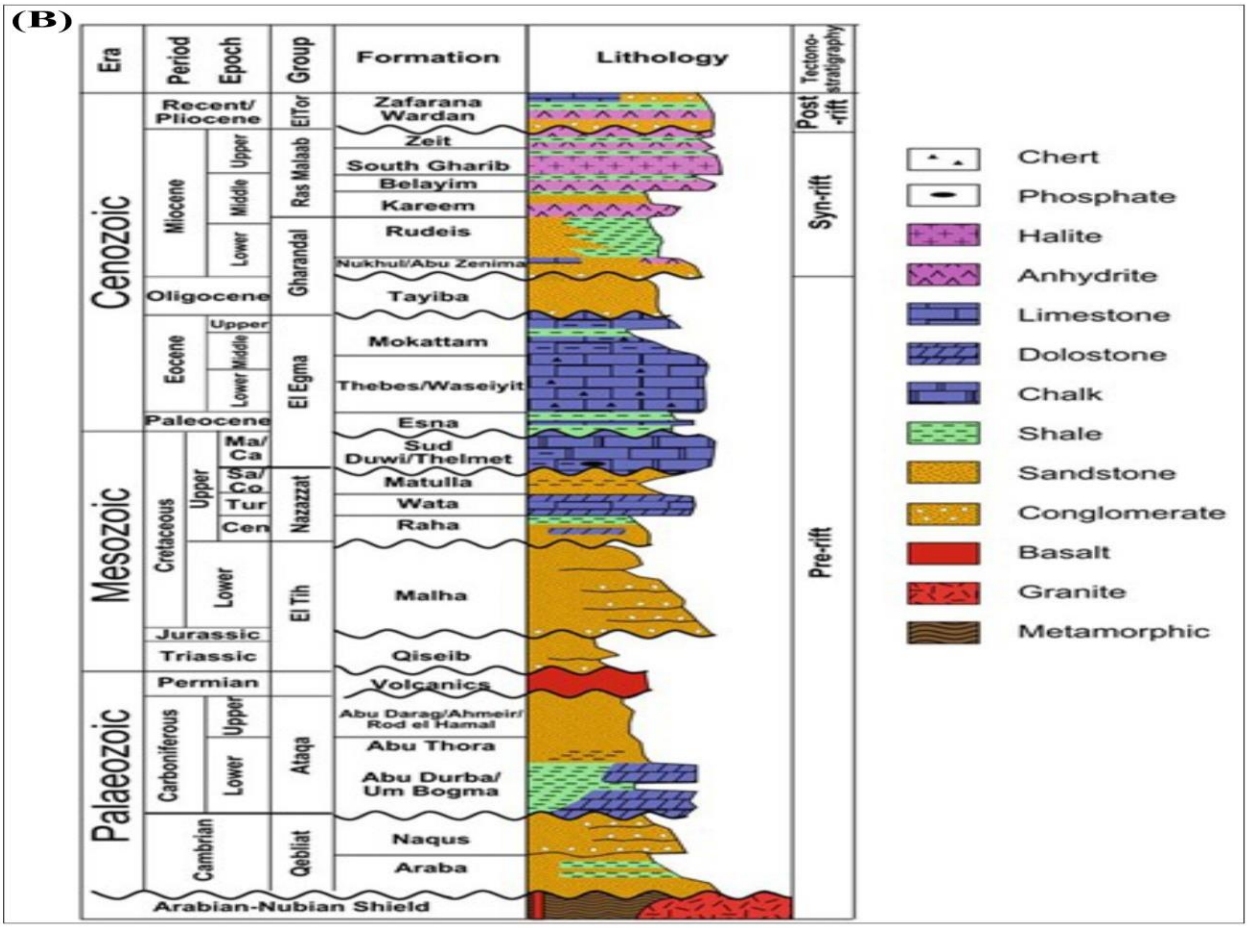

Fig. 2: (A) Geologic Map (modified after EGSMA, UNESCO, 2005) and (B) Stratigraphic column of the study area (after Pivnik et al., 2003).

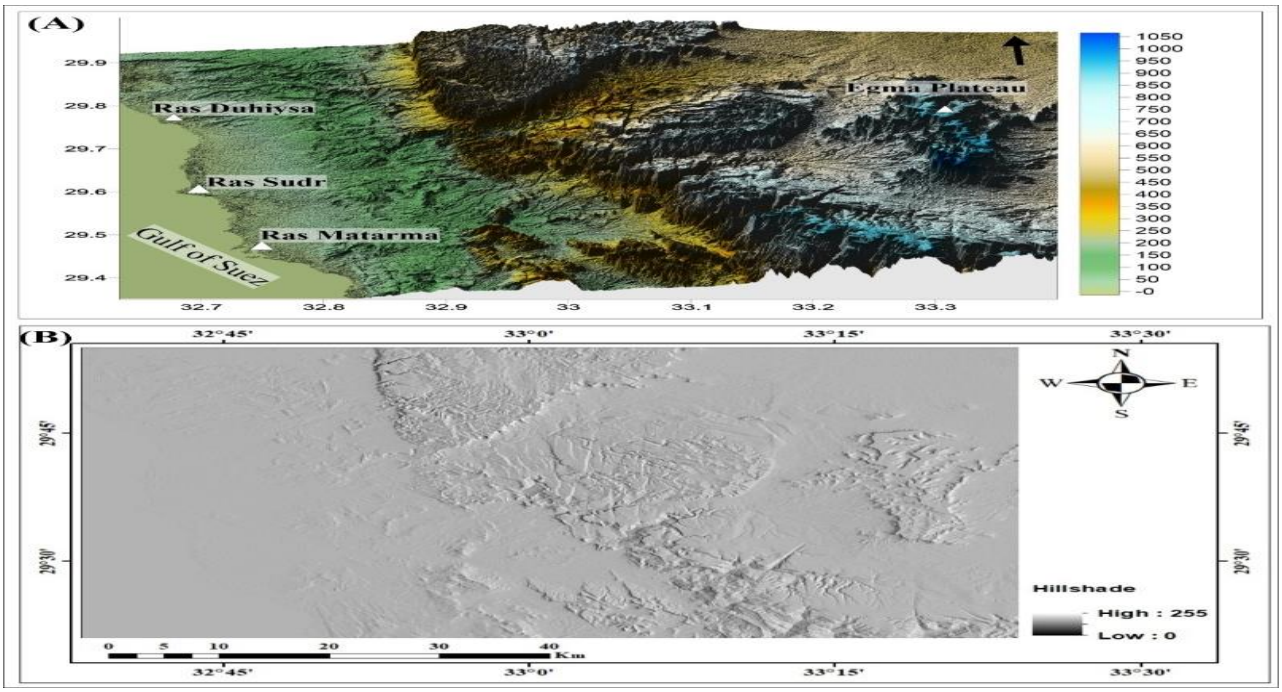

Fig. 3: (A) Digital elevation model and (B) Hillshade map of the study area.

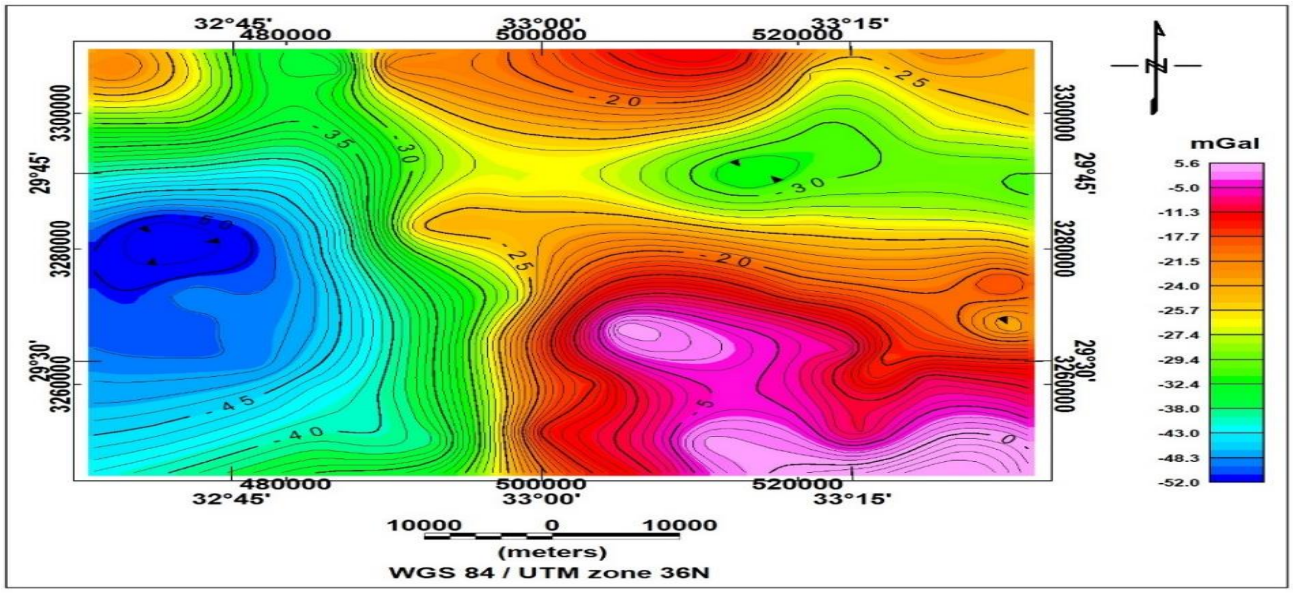

Fig. 4: Bouguer Anomaly Map.

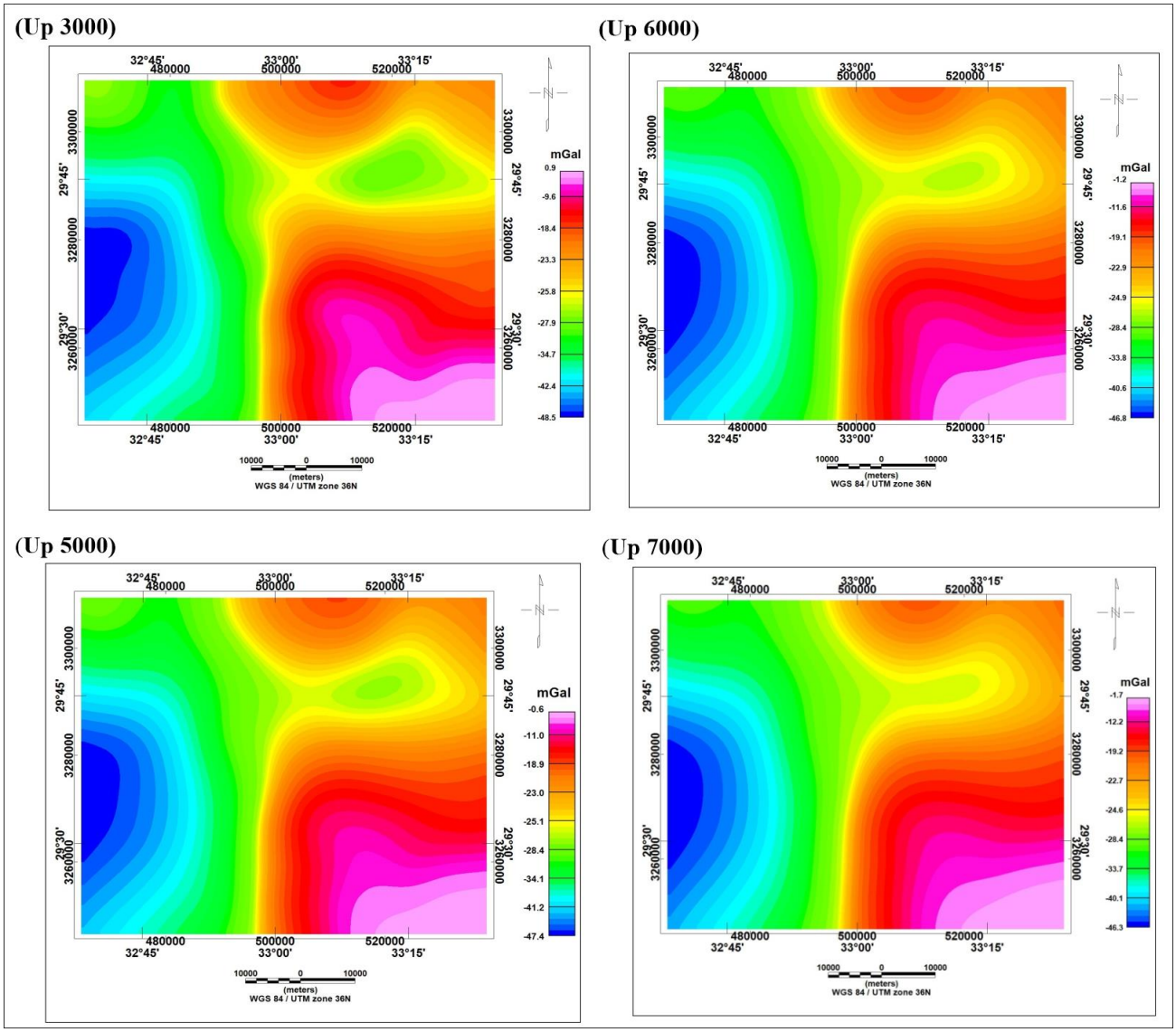

Fig. 5: Upward continuation gravity anomaly maps.

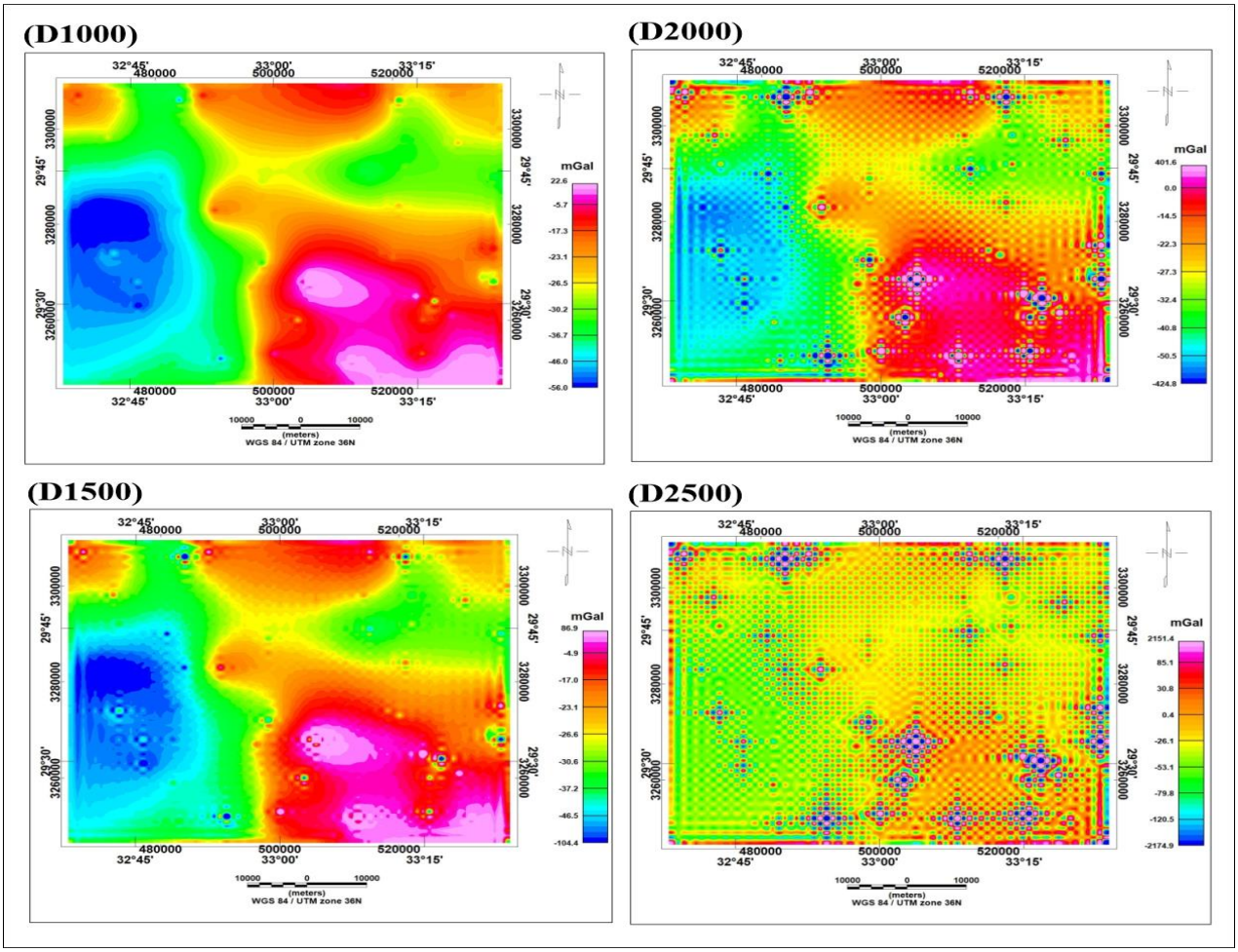

Fig. 6: Downward continuation gravity anomaly maps.

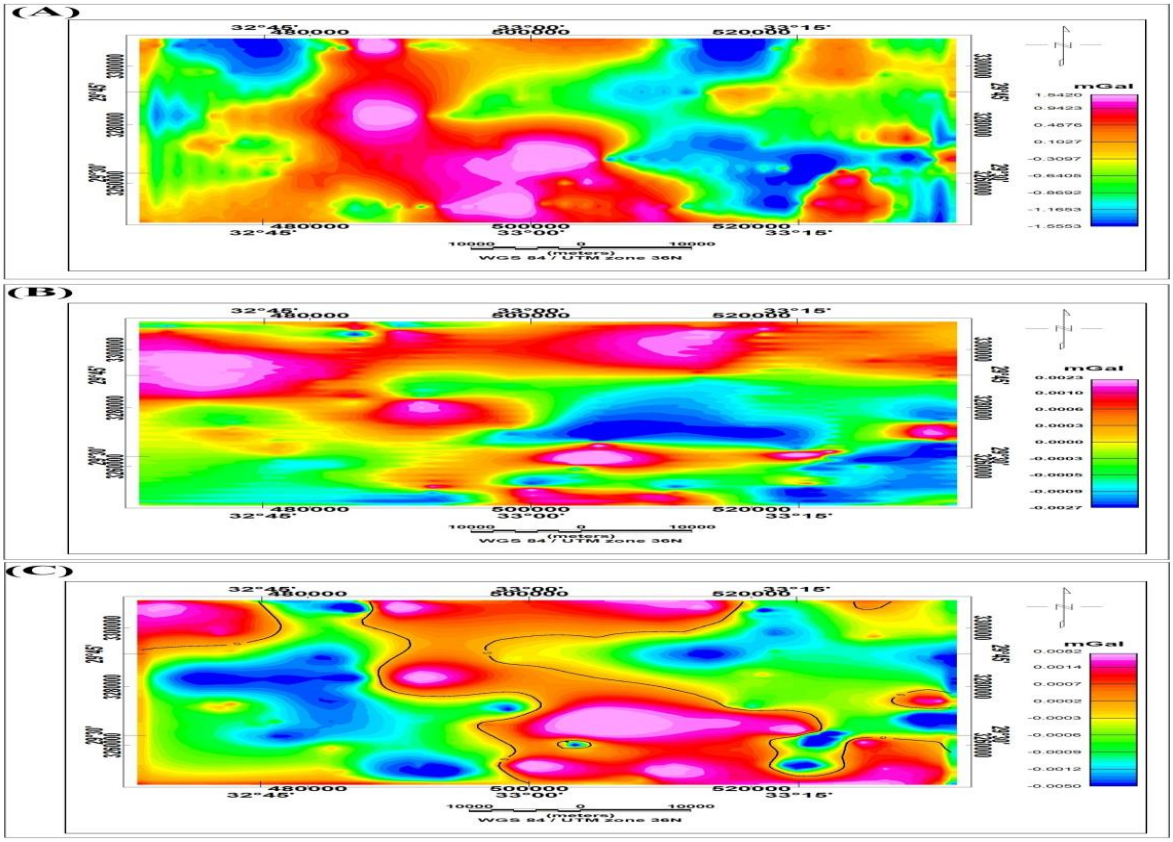

Fig. 7: (A), (B), (C) represent first derivatives in X, Y, Z directions and (D), (E), (F) represent second derivatives in X, Y and Z directions respectively of gravity anomaly maps.

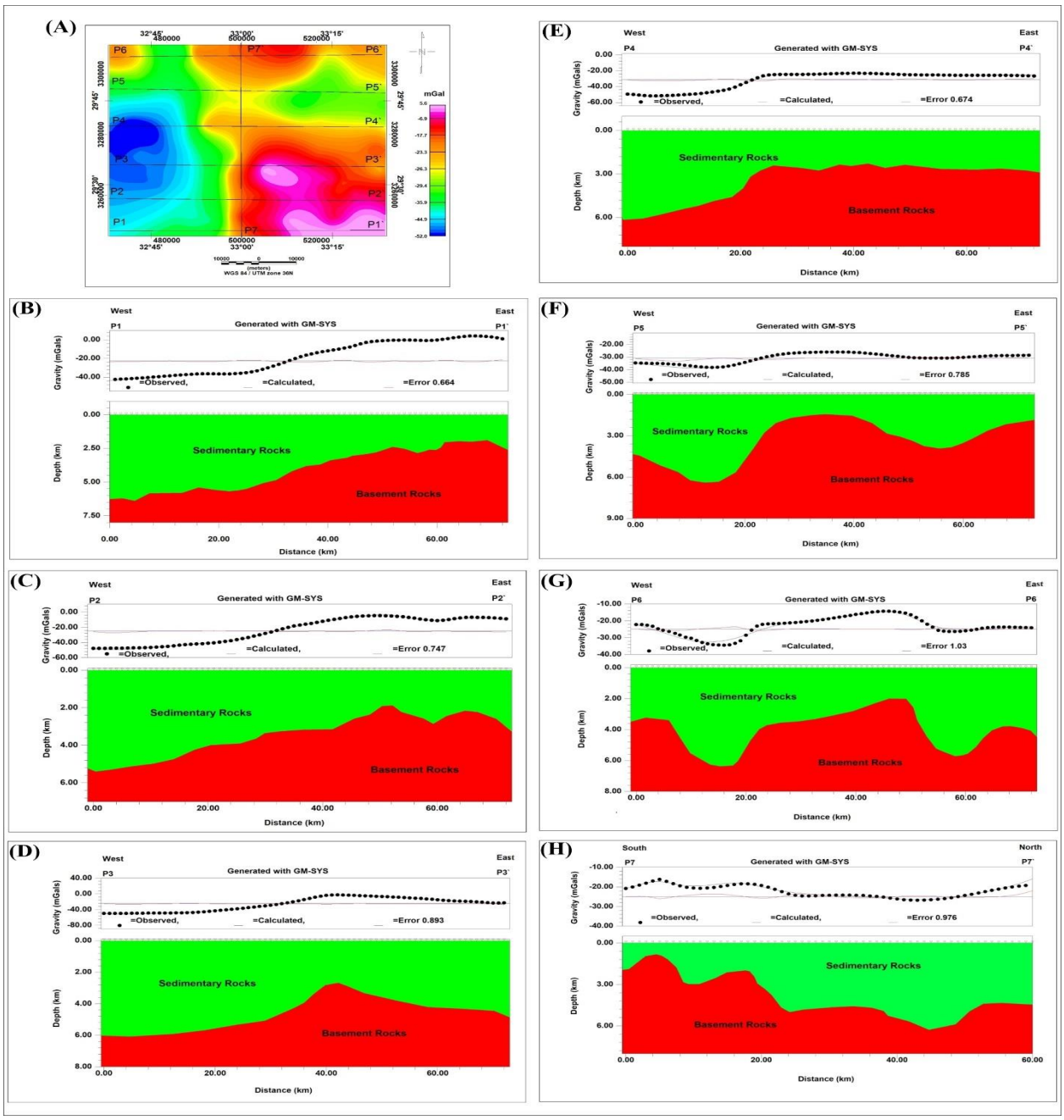

Fig. 8: (A) The distribution of the 2D profiles over the area. (B to H) show two-dimensional gravity modeling across the seven profiles.

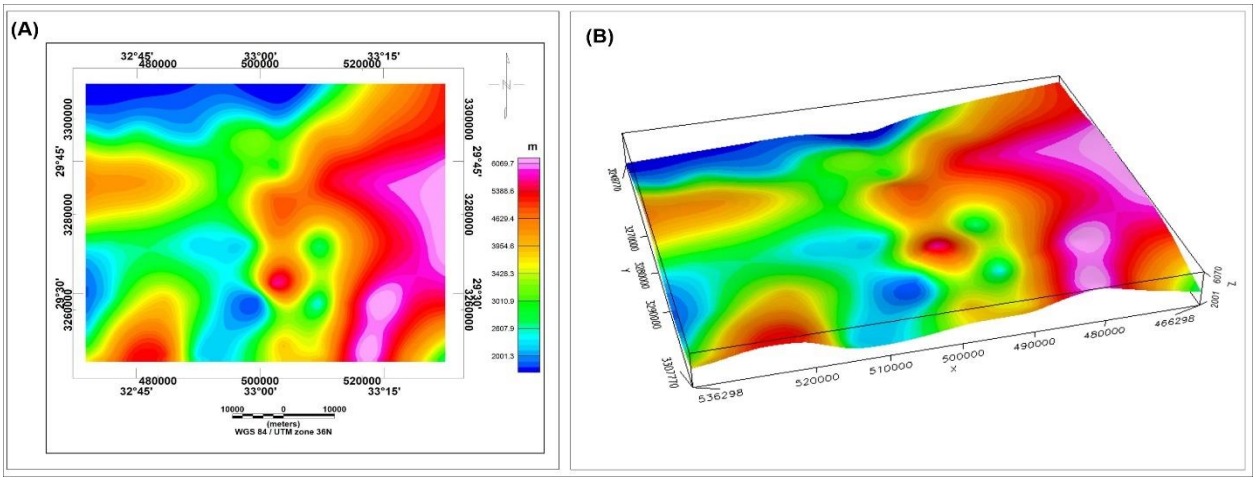

Fig. 9: (A) Map of the basement relief over the area where (B) shows 3D representation of the basement relief gravity map.

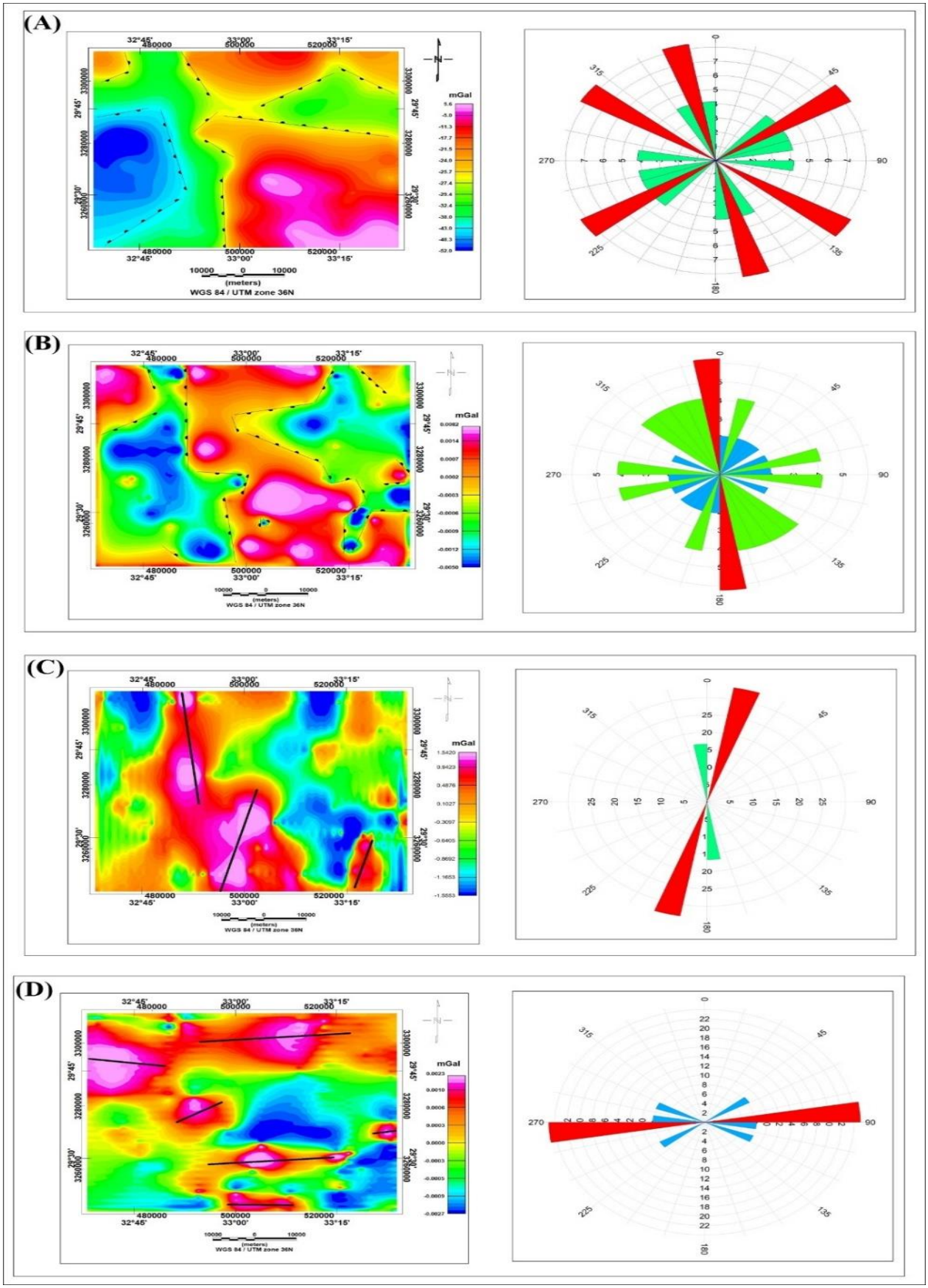

Fig. 10: Delineated lineaments from gravity data and corresponding rose diagrams; (A) From Bouguer anomaly map, (B) From FVD, (C) From FHD in X-direction, and (D) From FHD in Y-direction.

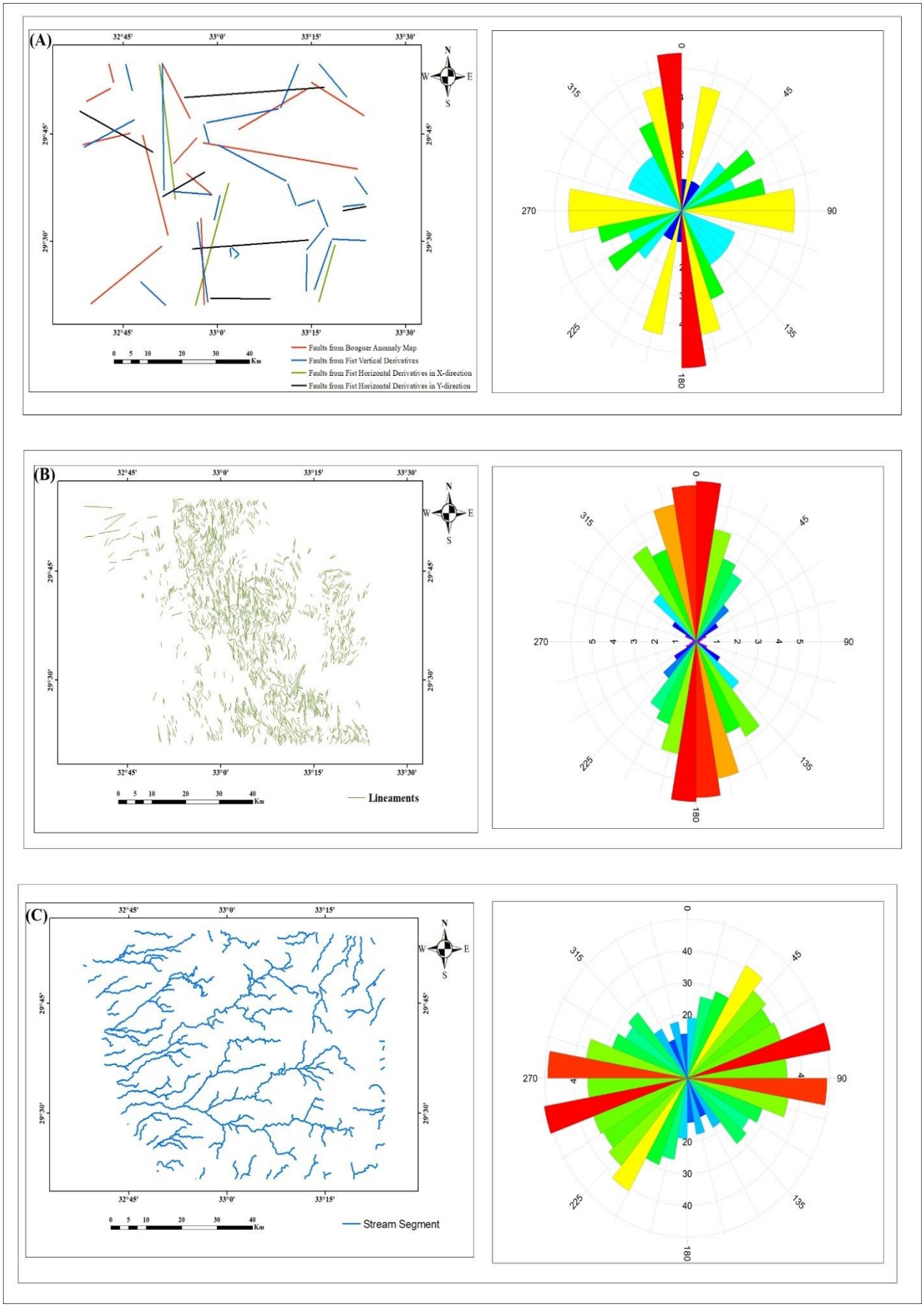

Fig. 11: (A) Total extracted lineaments over the area using gravity data, (B) Lineaments from hillshade map and its rose diagram. (C) Drainage map showing stream segments and its rose diagram.

7. References

1. Milsom, J; (1989): Field Geophysics; printed in Great Britian by Butler & Tanner Ltd, from and London, 232 p.
2. Shebl, A., & Csámer, Á. (2021). Reappraisal of DEMs, Radar and optical datasets in lineaments extraction with emphasis on the spatial context. Remote Sensing Applications: Society and Environment, **24**, 100617.
3. El-Bihery, M. A. (2009). Groundwater flow modeling of quaternary aquifer Ras Sudr, Egypt. Environmental geology, **58(5)**, 1095-1105.
4. Rabeh, T. (2011). Tectonic model of the Sinai Peninsula based on geophysical investigations. Tectonics. Fac. of Sci. Lisbon University, Portugal, 93-100.
5. Araffa, S. A. S., El-bohoty, M., Abou Heleika, M., Mekkawi, M., Ismail, E., Khalil, A., & Abd EL-Razek, E. M. (2018).
6. Implementation of magnetic and gravity methods to delineate the subsurface structural features of the basement complex in central Sinai area, Egypt. NRIAG *Journal of Astronomy and Geophysics*, **7(1)**, 162-174.
7. Elbarbary, S., Araffa, S. A., El-Shahat, A., Zaher, M. A., & Khedher, K. M. (2021). Delineation of water potentiality areas at Wadi El-Arish, Sinai, Egypt, using hydrological and geophysical techniques. *Journal of African Earth Sciences*, **174,** 104056.
8. EGSMA, NARSS, UNDP, UNESCO (2005). Project for the Capacity Building of The Egyptian Geological Survey and Mining Authority and The National Authority for Remote Sensing and Space Sciences in Cooperation with UNDP and UNESCO EGY/97/011.
9. Shata, A. (1955). Geomorphological aspects of the western Sinai foreshore. Bull. De l'Institute due desert, 5.
10. Said R (1991) The geology of Egypt. Elsevier publishing Co., Amsterdam, p 377
11. Oasis Montaj Program v.8.4, (2015). Geosoft mapping and processing system, version 8.4, 2015.
12. Fairfield, J., & Leymarie, P. (1991). Drainage networks from grid digital elevation models. Water resources research, **27(5)**, 709-717.
13. Blakely, R. J. (1996). Potential theory in gravity and magnetic applications. Cambridge University Press.
14. Yarger, H. L. (1985). Kansas basement study using spectrally filtered aeromagnetic data. In The utility of regional gravity and magnetic anomaly maps (pp. 213-232). Society of Exploration Geophysicists.
15. Blakely, R. J., & Simpson, R. W. (1986). Approximating edges of source bodies from magnetic or gravity anomalies. Geophysics, **51(7)**, 1494-1498.
16. Narayan, S., Sahoo, S. D., Pal, S. K., Kumar, U., Pathak, V. K., Majumdar, T. J., & Chouhan, A. (2017). Delineation of structural features over a part of the Bay of Bengal using total and balanced horizontal derivative techniques. Geocarto international, **32(4)**, 351-366.
17. Odek, A., Otieno, A. B., Ambusso, W. J., & Githiri, J. G. (2013). 2D-euler deconvolution and forward modeling of gravity data of Homa-hills geothermal prospect, *Kenya. Journal of Agriculture, Science and Technology*, **15(1),** 102-113.
18. Awad, M. S., El Kadi, H. H., Abbas, A. M., & Awad Sultan Araffa, S. (2022). Delineation of subsurface structures using gravity interpretation around Nabaa Al Hammara area, Wadi El Natrun, *Egypt. NRIAG Journal of Astronomy and Geophysics*, **11(1),** 282-292.
19. Araffa, S. A. S., Sabet, H. S., & Gaweish, W. R. (2015). Integrated geophysical interpretation for delineating the structural elements and groundwater aquifers at central part of Sinai Peninsula, *Egypt. Journal of African Earth Sciences*, **105,** 93-106.